Available online at www.sciencedirect.com
ScienceDirect
Trans. Nonferrous Met. Soc. China 33(2023) 3439−3451
Transactions of Nonferrous Metals Society of China
www.tnmsc.cn

Preparation of Pd membrane with high permeability and thermal stability on porous YSZ-Al_2O_3 tubes by two-step CeO_2 modification

Yu-xin YANG[1], Xin-zhong LI[1,2], Xiao LIANG[2], Rui-run CHEN[1], Jing-jie GUO[1], Heng-zhi FU[1], Dong-mei LIU[3]

1. School of Materials Science and Engineering, Harbin Institute of Technology, Harbin 150001, China;
2. School of Iron and Steel, Soochow University, Suzhou 215000, China;
3. Otto Schott Institute of Materials Research, Friedrich-Schiller-Universität Jena, Jena 07743, Germany

Received 20 May 2022; accepted 30 August 2022

Abstract: Pd membranes were deposited on porous YSZ-Al_2O_3 tubes after different modification methods using an electroless plating technology. SEM, AFM, XRD and gas permeation tests were applied to investigating the effects of different modification methods on the surface quality of porous tubes and the permeation performance of the Pd composite membranes. The results showed that the surface of the porous tubes after the two-step CeO_2 modification exhibited smaller pore distribution and roughness. Pd membranes on the porous tubes after the two-step CeO_2 modification exhibited higher hydrogen permeation flux (0.549 $mol \cdot m^{-2} \cdot s^{-1}$) and H_2/N_2 selectivity (14241) at 500 °C and a pressure difference of 700 kPa. The results of different thermal cycling tests and the long-term permeation tests of 1000 h showed that Pd membranes on the porous tubes after the two-step CeO_2 modification had higher permeation stability.

Key words: hydrogen separation; Pd membrane; porous tube; surface modification; CeO_2

1 Introduction

Pd and its alloys (such as Pd−Ag) are the commonly used membrane materials for hydrogen separation and purification due to their high selectivity, high hydrogen permeability, and excellent chemical compatibility [1,2]. However, the high cost of Pd is a severe limitation [3]. The current self-supporting Pd foils for commercial applications are typically thicker than 50 μm, which results in the high cost and the low hydrogen permeation flux. The hydrogen flux is linear with the inverse of thickness of Pd membrane. Accordingly, there is a great demand for the development of Pd membrane with ever-decreasing thickness. Much current research focused on the preparation of Pd/porous support composite membranes, in which a thin Pd membrane was deposited on a porous support [4−7]. The composite membranes exhibit advantages such as low Pd consumption, high hydrogen permeability and facile module construction, which are considered to be promising candidates to commercial rolled Pd foils [8,9].

Among various technologies, electroless plating is the commonly used method to prepare Pd membranes in terms of simple equipment, cost performance and deposition on all kinds of substrates [10−13]. Among various support materials, porous ceramic is attractive due to its wide market availability, low cost and high chemical stability. The preparation of dense Pd membranes is largely affected by the surface quality of the ceramic supports [14]. The surface of commercial porous ceramic tubes exhibits the

Corresponding author: Xin-zhong LI, Tel: +86-15862396657, E-mail: lixz@suda.edu.cn;
Dong-mei LIU, Tel: +49-15778465623, E-mail: dongmei.liu@uni-jena.de
DOI: 10.1016/S1003-6326(23)66345-9

uneven distribution of pore sizes, with some large pores and large roughness. Therefore, surface modification for the porous ceramic is critical importance prior to the deposition of Pd membranes. Surface modification usually involves coating materials (such as Al_2O_3 [15−17], ZrO_2 [18,19], YSZ [20,21], TiO_2 [22,23], CeO_2 [24−26], and SiO_2 [27]) on the surface of porous supports to reduce the pore sizes and roughness. The material selection for surface modification is a key of interest due to the large difference of the thermal expansion coefficients between Pd and porous ceramic. The thermal expansion coefficient of CeO_2 (1.1×10^{-5} K^{-1}) is the closest to that of Pd (1.2×10^{-5} K^{-1}) compared to that of other oxides. Moreover, a series of studies [25,26,28] have demonstrated that Pd/CeO_2/porous support composite membranes generally exhibit high thermal stability during the long-term permeation. In addition, the surface modification methods also affect the selectivity and hydrogen permeance of the Pd composite membranes. TONG et al [24] used CeO_2 particles with an average particle size of micron-scale to modify the surface of porous stainless steel and subsequently prepared the Pd membrane (~10 μm), but the selectivity of composite membrane was only 108. TERRA et al [29] found that hydrogen permeation flux of the Pd membrane (~1.81 μm) on a graphite modified porous Al_2O_3 support was close to that of Pd membrane (~2.41 μm) on a support without surface modification, which implies that surface modification is resistant to hydrogen transport. Therefore, the detailed manufacturing steps of the surface modification for porous supports should be optimized to increase the selectivity and reduce mass transfer resistance. Recently, CHI et al [15] put forward a two-step method using Al_2O_3 particles (sizes of ~10 and ~1 μm, respectively) for surface modification of porous stainless steel tubes. It is found that the two-step Al_2O_3 modification contributes significantly to the subsequent preparation of a dense Pd membrane with high hydrogen permeance.

At present, the effects of CeO_2 modification on the surface of porous YSZ-Al_2O_3 tubes and the performance of Pd composite membranes have not been elucidated. In this work, the surface of porous YSZ-Al_2O_3 tubes was modified by different methods and then Pd membranes were prepared on different porous tubes. The effects of different modification methods on the surface quality of the porous YSZ-Al_2O_3 tubes were investigated, and the effects of different modification methods on the hydrogen permeation behaviors and thermal stability of different Pd composite membranes were also studied.

2 Experimental

2.1 Membrane preparation

A commercial porous YSZ-Al_2O_3 tube (12 mm in outer diameter, 8 mm in inter diameter, and 500 mm in length) was cut into short tubes (130 mm in length) as the supports. The porous tubes were cleaned using NaOH solution and deionized water in order to remove contaminants, and then were dried at 120 °C in an oven for 2 h. Figure 1 shows the schematic process of the two-step CeO_2 modification for the surface of a porous

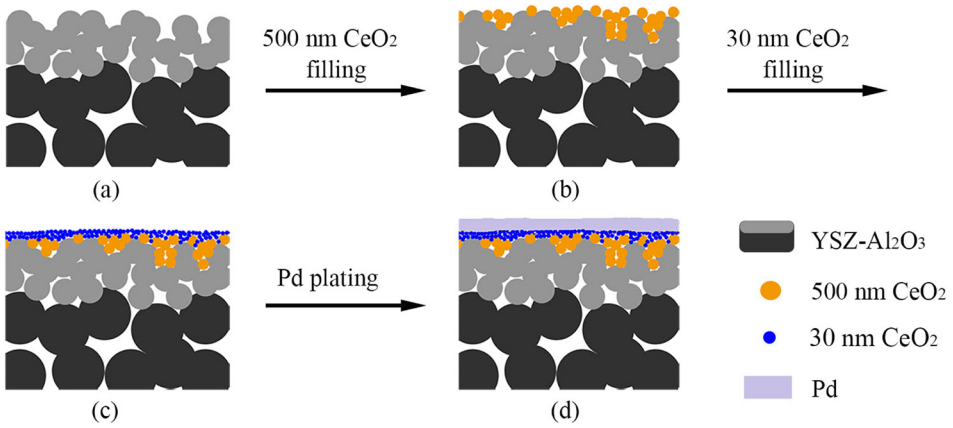

Fig. 1 Schematic process of two-step CeO_2 modification for surface of porous YSZ-Al_2O_3 tube and preparation of Pd membrane

YSZ-Al_2O_3 tube. 500 nm CeO_2 particles and 30 nm CeO_2 particles were used to successively modify the surface pore size and roughness of the tube and then Pd membrane was deposited on the tube after surface modification.

A vacuum-assisted technique was used to conduct the two-step CeO_2 modification for the porous YSZ-Al_2O_3 tube. The CeO_2 particles were fabricated by Zhonghang Nano. Tech. Dev. Co., China. Firstly, a suspension of CeO_2 particles (average size of 500 nm) was prepared with a CeO_2 concentration of ~0.2 wt.% in water. The porous tube after inside sealing was dipped into the CeO_2 suspension and then the inside of the tube was vacuumed so that the CeO_2 particles in the suspension were incorporated into the pores of the surface of the porous tube. After about 10 min, the porous tube was taken out from the suspension. The inside of the porous tube remained vacuumed and a clean cloth was used to gently brush off the excessive CeO_2 particles adhered to the surface of the porous tube until no visible CeO_2 particles were present on the cloth. This ensures that the CeO_2 particles fill mainly into the pores on the surface of the porous tube, reducing the thickness of the modification layer and the resistance to penetration. The modified porous tube was placed in an oven and calcined at 500 °C for 3 h to ensure CeO_2 stability and then cooled in air to room temperature. Then, the porous tube after surface modification with 500 nm CeO_2 particles was further modified using 30 nm CeO_2 particles. The modified process was similar to the above.

The Pd membrane was deposited on the modified porous YSZ-Al_2O_3 tube using the electroless plating technology. Prior to the deposition, the surface of the porous tube was activated by seeding with Pd nuclei through a sensitization/activation pre-treatment. The porous tube was sequentially immersed in $SnCl_2$ solution (1 g/L) for 2 min and $PdCl_2$ solution (0.1 g/L) for 2 min, with rinsing by deionized water for 30 s after each solution. The process was repeated 10 times until the porous tube surface exhibited a uniform dark brown color. After activation, the porous tube was placed into a Pd bath at 60 °C and rotated at a rate of 200 r/min in order to uniformly deposit Pd membrane by electroless plating. The compositions of the Pd bath included 5 g/L $PdCl_2$, 10 mL/L HCl (37%), 68 g/L EDTA, 250 mL/L $NH_3·H_2O$ (28%), and 0.75 mL/L $N_2H_4·H_2O$ (50%). To prevent the bulk precipitation of Pd in the bath at 60 °C, the bath was changed every 3 h and the reducing agent ($N_2H_4·H_2O$) was added batch wise into the bath. Pd membranes (with thickness of ~14 μm) were deposited on the modified porous YSZ-Al_2O_3 tubes by controlling the time of electroless plating. For comparison, Pd membrane with similar thickness was deposited on the pristine porous tube (without surface modification). Table 1 shows the preparation conditions of four composite membranes, named M1, M2, M3, and M4. The thicknesses of Pd membranes were determined gravimetrically and verified by SEM.

2.2 Membrane characterization

A scanning electron microscope (SEM, FEI-Quanta−250F, USA) equipped with energy diffraction X-ray (EDX) analysis was used to characterize the morphology of porous YSZ-Al_2O_3 tubes before and after modification using CeO_2 particles and the microstructure of the Pd/CeO_2/YSZ-Al_2O_3 composite membranes before and after the hydrogen permeation tests. The surface roughness of different porous tubes was characterized by AFM (Bruker Dimension Icon, USA). The X-ray diffraction analysis (XRD, MiniFlex−600, Rigaku, Japan) with the Cu K_α radiation at the step rate of 1 (°)/min (with the step size of 0.02°) in 2θ range of 20°−90° was used to characterize the constituent phase of Pd membranes.

Table 1 Preparation conditions of four composite membranes

Membrane	Modification	Method	Plating temperature/°C	Rotation rate/(r·min^{-1})	Plating time/h	d_{Pd}/μm
M1: Pd/YSZ-Al_2O_3	No	ELP	60	200	6	14.3
M2: Pd/CeO_2/YSZ-Al_2O_3	500 nm CeO_2	ELP	60	200	6	13.5
M3: Pd/CeO_2/YSZ-Al_2O_3	30 nm CeO_2	ELP	60	200	6	14.8
M4: Pd/CeO_2/YSZ-Al_2O_3	(500 nm + 30 nm) CeO_2	ELP	60	200	6	14

ELP represents the electroless plating technology; d_{Pd} is the thickness of Pd membrane

2.3 Permeation measurements

The hydrogen permeability and the thermal stability of the composite membranes (M1, M2, M3, and M4) were characterized using a gas permeation apparatus. The Swagelok fittings of 12 mm (I.D.) (code: SS-12M0-6) and graphite ferrules of 12 mm (I.D.) (purchased from Kainuo Sealing Co., China) were used to seal the membranes. The membrane was fitted to the connectors. The used torque for the sealing of the membrane was 15 N·m and the nitrogen leakage was lower than 0.01 mL/min at a pressure up to 1 MPa. Then, the sealed membrane was put into a stainless steel reactor. The reactor was heated under a N_2 atmosphere from room temperature to 350 °C at a rate of 2 °C/min in a furnace. At this temperature, the N_2 gas was evacuated and H_2 was introduced for permeation tests. H_2 flux was measured using a flow meter at pressure differences from 50 to 700 kPa. Similar tests were conducted at 400, 450 and 500 °C, respectively. In order to evaluate the hydrogen permeation selectivity for each membrane, N_2 flux through the membrane was measured after each H_2 flux test in the same condition. Two kinds of thermal cycling tests and a long-term permeation operation were used to determine the permeation stability for each membrane. One thermal cycling test was changing the temperature between 350 and 500 °C, and the H_2 flux was measured at each individual temperature. The other thermal cycling test was that the membrane suffered from a thermal cycling between room temperature and 500 °C and the H_2 and N_2 flux levels at 500 °C were measured for each cycle. The thermal stability of the membrane can be evaluated by comparing the difference in H_2 and N_2 flux per cycle. The long-term permeation operation was carried out at 500 °C for 1000 h. During the above tests, the pressure difference between both sides of the membrane was kept at 100 kPa.

3 Results and discussion

3.1 Morphology and roughness of porous YSZ-Al_2O_3 tubes

Figures 2(a)−(d) show the surface, radial direction morphology and roughness of a pristine porous YSZ-Al_2O_3 tube. Rough and uneven surface with some defects (such as large-size pores) can be observed. Although the nominal pore size is ~50 nm, some of the pores on the surface are over 10 μm in size. It is difficult to prepare a thin and pinhole-free Pd membrane directly on the porous YSZ-Al_2O_3 tube. Surface modification for the porous tube is necessary to reduce the surface defects, roughness and pore-mouth sizes. Herein, CeO_2 particles of two different sizes (500 and 30 nm, respectively) are used to modify the porous tube. The 500 nm CeO_2 particles are larger than the nominal pore size of the porous tube that can prevent the particles from entering the interior of the porous tube. The 500 nm CeO_2 particles are used to fill the large pores on the surface and 30 nm CeO_2 particles are expected to decrease the surface roughness.

Figures 2(e)−(h) show the surface, radial direction morphology and roughness of the porous YSZ-Al_2O_3 tube modified with 500 nm CeO_2 particles. Many large pores on the surface are largely reduced as compared to those without modification, but there are still some defects of submicron sized pores. Localized protrusions can be observed on the surface and the surface roughness is still large. After modification with 500 nm CeO_2 particles, the value of root mean square roughness (R_q) is reduced by ~54% compared with that of the pristine tube. Figures 2(i)−(l) show the surface, radial direction morphology and roughness of the porous tube modified with 30 nm CeO_2 particles. There are a few defects of submicron sized pores on the surface, and local surface is smoother than that modified with 500 nm CeO_2 particles, but there are still some localized protrusions. The value of R_q was reduced by ~61% compared with that of the pristine tube. Figures 2(m)−(p) show the surface, radial direction morphology and roughness of the porous tube modified with 500 nm and 30 nm CeO_2 particles successively. It can be seen that the two-step modification largely reduces the surface defects and roughness and improves the surface quality of the tube. The value of R_q is reduced by ~78% compared with that of the pristine tube. This can be attributed to that the porous tube is first modified with 500 nm CeO_2 particles to reduce the large pore-mouth sizes on the tube surface, followed by modification using 30 nm CeO_2 particles to further smoothen the surface.

Surface modification with CeO_2 particles for the porous tube largely improves the surface quality, but it may create a resistance to the gas permeation

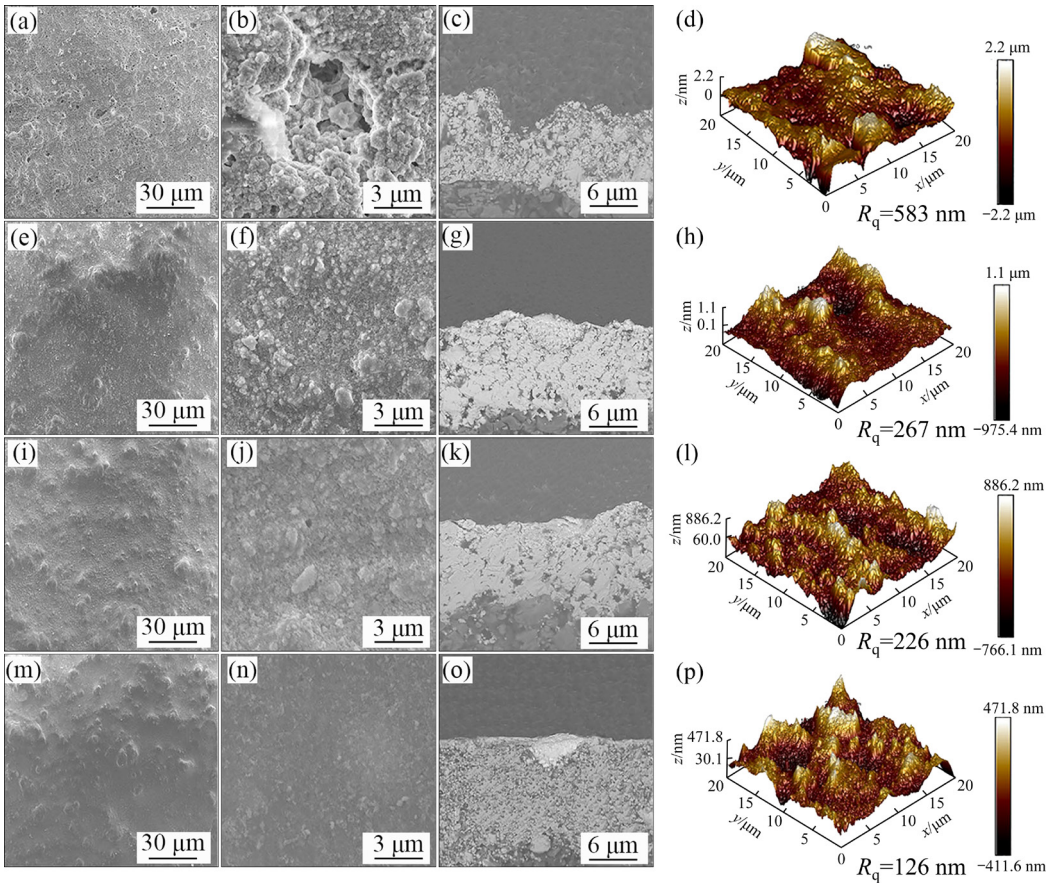

Fig. 2 SEM images of surface (a, b, e, f, i, j, m, n), radial direction morphology (c, g, k, o), and AFM images showing surface roughness (d, h, l, p) of porous YSZ-Al_2O_3 tubes: (a−d) Pristine state; (e−h) After modification with 500 nm CeO_2 particles; (i−l) After modification with 30 nm CeO_2 particles; (m−p) After modification with 500 nm and 30 nm CeO_2 particles successively

through the tube. To evaluate the mass transfer resistance, H_2 and N_2 permeation tests were performed for different tubes. The selectivity of tube is the ideal H_2/N_2 selectivity and is calculated from the ratio of the permeation flux of H_2 to N_2. Figure 3 shows the gas permeation flux and selectivity through different tubes. It can be seen that the H_2 flux through the tube after modification with 500 nm CeO_2 particles decreases to ~89% that of the pristine tube. After modification with 30 nm CeO_2 particles, the H_2 flux through the tube decreases to ~80% that of the pristine tube. Large particles mainly fill into the pore mouths near the surface, resulting in minor blockage of flow passages of the tube. In contrast, fine particles fill into the inside pore passages of the tube that blocks the gas flow. After modification with 500 nm and 30 nm CeO_2 particles successively, the H_2 flux through the tube decreases to ~88% that of the pristine tube. This is close to that after modification

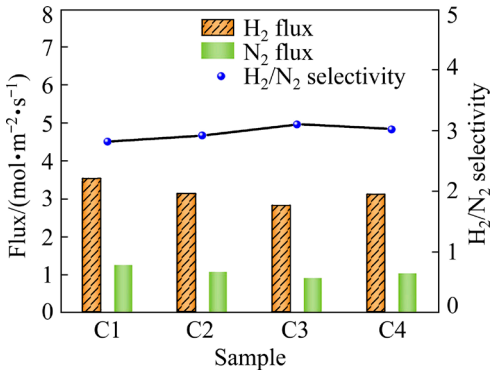

Fig. 3 Gas permeation flux and selectivity through different porous YSZ-Al_2O_3 tubes at 500 °C and pressure difference of 50 kPa: C1 (the pristine one); C2 (after modification with 500 nm CeO_2 particles); C3 (after modification with 30 nm CeO_2 particles); C4 (after modification with 500 nm and 30 nm CeO_2 particles, successively)

with 500 nm CeO_2 particles only, because the 500 nm CeO_2 particles at the surface pore mouths

would help to prevent the 30 nm CeO_2 particles from filling the inside passages of the tube and make the 30 nm CeO_2 particles evenly distribute on the surface. The H_2/N_2 selectivity through the tube increased with the surface modification and reached ~3 after the two-step modification which was close to the value of Knudsen diffusion [30].

3.2 Microstructure of Pd composite membranes

A thin Pd membrane was deposited on the porous YSZ-Al_2O_3 tube after a two-step CeO_2 modification using an electroless plating technology. The Pd membrane was composed of densely arranged Pd clusters (see Figs. 4(a) and (b)) and there were no obvious pinhole defects. Figure 4(c) shows the radial microstructure of the composite membrane. Bright Pd membrane, thin CeO_2 intermediate layer, YSZ layer on top of the porous tube and Al_2O_3 layer of the porous tube can be observed. The Pd membrane was closely bound to the CeO_2 intermediate layer and its thickness (~14 μm) was generally the same. CeO_2 particles were mainly filled into the large-size pores on the surface of the porous tube and thus the thickness of the resulted CeO_2 intermediate layer was not uniformly distributed which was extremely thin on the surface and thicker in the large-size pores of the tube. The YSZ layer (~15 μm) exhibited much smaller pore sizes than the Al_2O_3 layer (~2 mm). This kind of structure of YSZ-Al_2O_3 tube provides high porosity with small average pore sizes. Figure 4(d) shows the XRD pattern of the Pd membrane on the composite membrane. The membrane consisted of reflection peaks of Pd. The reflection peaks of CeO_2, YSZ and Al_2O_3 did not appear.

3.3 Hydrogen permeation performance of Pd composite membranes

Hydrogen permeation tests were conducted for the four composite membranes (M1, M2, M3, and M4 in Table 1) at 350−500 °C under pressure differences from 50 to 700 kPa. Figure 5 shows the dependence of hydrogen permeation flux through each membrane on pressure difference at four temperatures. The hydrogen flux (J) is directly

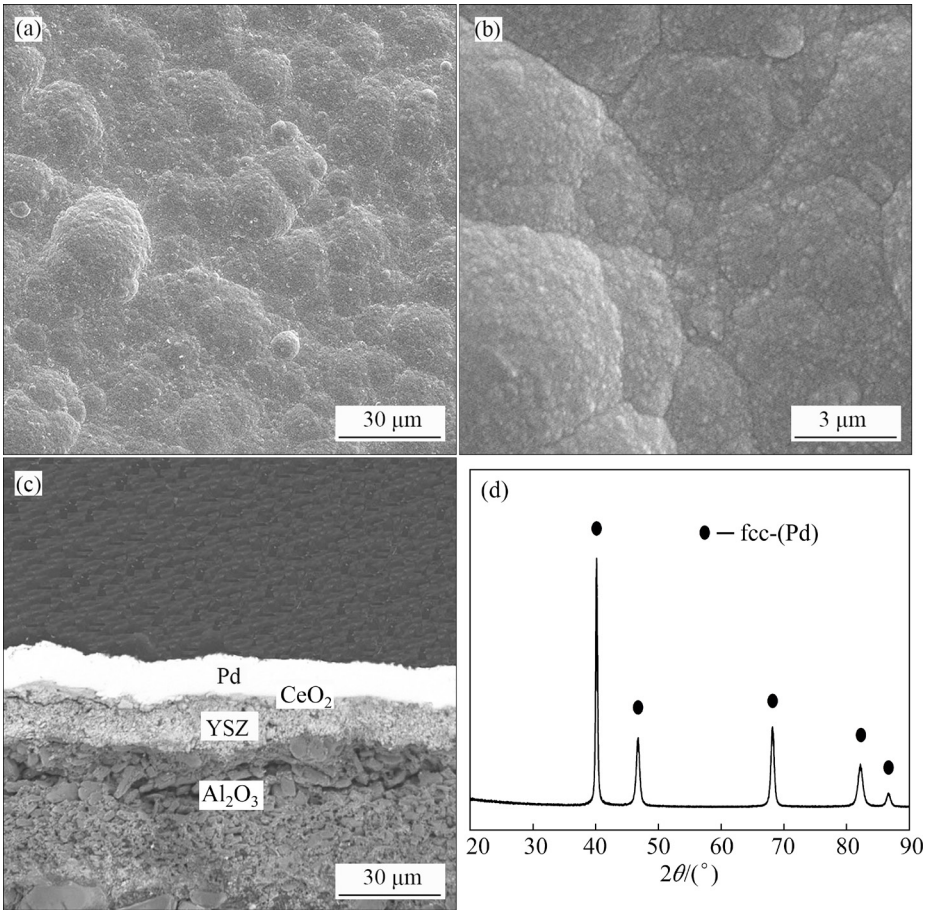

Fig. 4 SEM images of Pd/CeO_2/YSZ-Al_2O_3 composite membrane on surface (a, b) and in radial direction (c), and XRD pattern of Pd membrane on composite membrane (d)

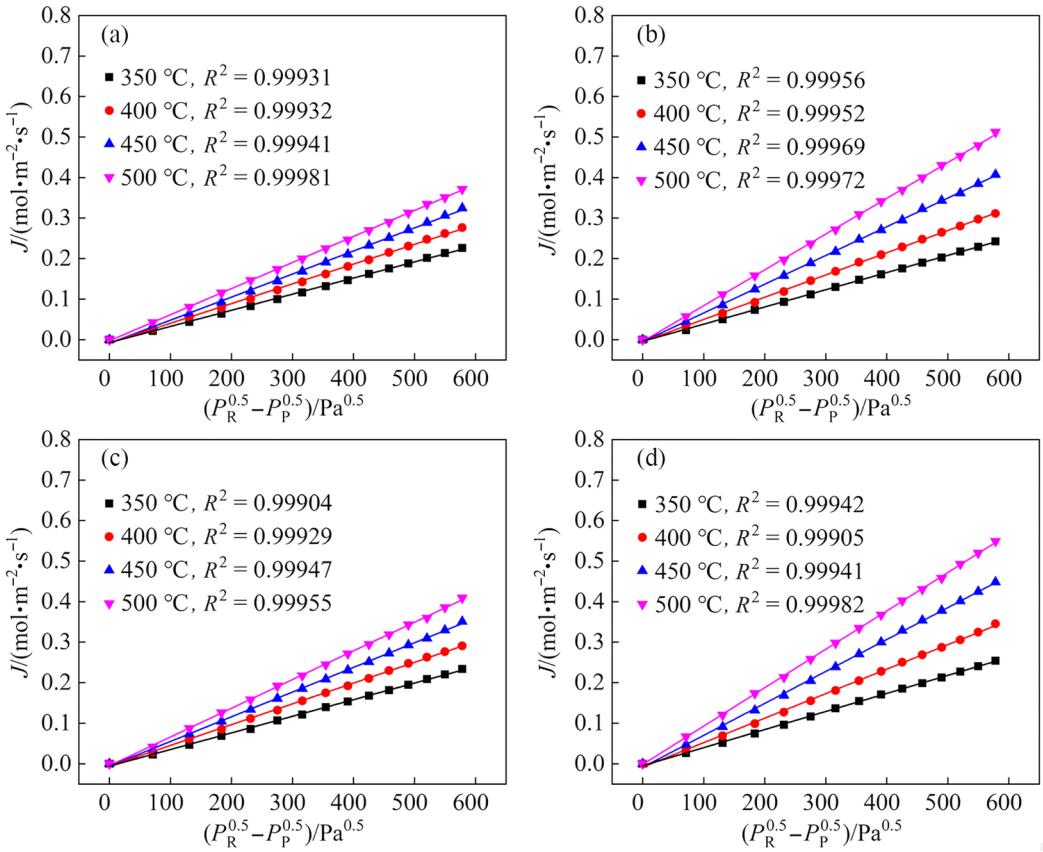

Fig. 5 Hydrogen permeation flux (J) through M1 (a), M2 (b), M3 (c), and M4 (d) as function of ($P_R^{0.5}$–$P_P^{0.5}$) at 350−500 °C

proportional to the difference of the square roots of the hydrogen pressures on each side of the membrane. This implies that the hydrogen permeation kinetics obeys Sieverts' law [31]. For each membrane, the J value increased with the increase of temperature and pressure difference between both sides of the membrane. The M4 exhibited the highest J value and the M1 exhibited the lowest one under the same condition. Typically, the J values of M4, M3, M2 and M1 were 0.549, 0.409, 0.512, and 0.372 mol·m^{-2}·s^{-1} at 500 °C under a pressure difference of 700 kPa, respectively.

For the Pd/porous support composite membranes, the hydrogen permeation flux can be expressed as follows [6]:

$$J=\frac{\Phi}{d_{Pd}}(P_R^n-P_P^n) \quad (1)$$

where Φ is the hydrogen permeability, n is the pressure exponent, and P_R and P_P are the hydrogen pressures on the retentate and permeate sides, respectively. The hydrogen permeability Φ for four composite membranes at different temperatures was obtained, as shown in Table 2. The Φ value increased with the increase of temperature for each membrane. The M4 exhibited the highest Φ value among four composite membranes at the same temperature. Typically, at 500 °C, the Φ value of M4 was 13.2×10^{-9} mol·m^{-1}·s^{-1}·Pa$^{-0.5}$, which was ~1.5 times that of M1, ~1.1 times that of M2, and ~1.4 times that of M3. Different hydrogen permeability values may be related to the structure of Pd composite membranes. In M1, the Pd membrane was deposited directly on the porous tube and some of Pd appeared the inside of the pores of the tube. This maybe induce an additional resistance to hydrogen permeation process or reduce effective membrane area on the permeate side. In contrast, in M4, the Pd membrane was deposited on the porous tube after two-step modification, and the CeO_2 intermediate layer may hinder massive Pd into the pores. MARTINEZ-DIAZ et al [25] found that the excessive deposition of Pd into the pores of the porous support would induce an additional resistance to hydrogen permeation process. WEI et al [32] found that

surface modification for porous ceramic support by TiO_2 increased the effective membrane area on the permeate side and improved the hydrogen permeability of the Pd/TiO_2/porous ceramic composite membranes. Correspondingly, the hydrogen permeability of the M4 was higher than that of the M1. Compared with the two-step modification, the surface after 500 nm CeO_2 modification still exhibited some submicron sized pores, resulting in the deposition of some Pd into the pores. Thus, the hydrogen permeability of the M2 was slightly lower than that of the M4. The porous tube after 30 nm CeO_2 modification exhibited large permeation resistance, resulting in that the hydrogen permeability of the M3 was lower than that of the M4 and M2 but slightly higher than that of the M1.

Table 2 Hydrogen permeability of four composite membranes at different temperatures

Membrane	$\Phi/(10^{-9}$ mol·m^{-1}·s^{-1}·Pa$^{-0.5})$			
	350 °C	400 °C	450 °C	500 °C
M1: Pd/YSZ-Al_2O_3	5.13	6.31	7.43	8.83
M2: Pd/CeO_2/YSZ-Al_2O_3	5.65	7.36	9.6	12.1
M3: Pd/CeO_2/YSZ-Al_2O_3	5.36	6.79	8.14	9.58
M4: Pd/CeO_2/YSZ-Al_2O_3	6.01	7.94	10.5	13.2

During the hydrogen permeation process of the Pd composite membranes, pinhole defects may appear in the Pd membrane due to the growth of Pd grains, which reduce the selectivity [33,34]. To evaluate this selectivity, N_2 permeation tests were performed for four composite membranes after H_2 permeation tests at 350, 400, 450 and 500 °C under a pressure difference of 700 kPa. The ratio of the permeation flux of H_2 to N_2 is the ideal H_2/N_2 selectivity of the composite membranes. Figure 6 shows the H_2/N_2 selectivity of M1, M2, M3, and M4. The selectivity increases with the increase of temperature for each membrane. Typically, the selectivity of M4 increases from 6642 to 14241 when the temperature increased from 350 to 500 °C under a pressure difference of 700 kPa. The N_2 flux decreases with increasing temperature because N_2 through the pinhole defects in the Pd membrane is mainly governed by Knudsen diffusion and viscous flow [35]. In contrast, the H_2 flux increases with increasing temperature because hydrogen permeation through the Pd membrane is mainly governed by the solution diffusion mechanism. Consequently, the selectivity of the composite membranes increases with the increase of temperature. At a fixed temperature, the M4 exhibited the highest hydrogen permeation selectivity and the M1 exhibited the lowest one. The two-step modification for the porous tube favors the preparation of a dense and even Pd membrane, which is less prone to pinhole defects during hydrogen permeation process, ensuring a high selectivity. In contrast, the Pd membrane in M1, deposited directly on the porous tube without surface modification, exhibits large difference in grains in the microstructure, which is prone to anomalous grain growth and pinhole formation at a relatively high temperature. The M2 and M3 exhibit higher selectivity than the M1 but lower than the M4 because the surface quality of porous tubes modified by the one-step method is higher than that of porous tubes without modification but lower than that of porous tubes modified by the two-step method.

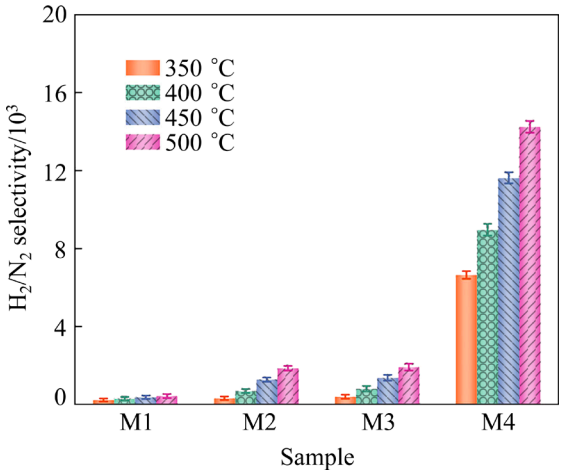

Fig. 6 Hydrogen permeation selectivity through M1, M2, M3 and M4 at 350−500 °C under pressure difference of 700 kPa

Table 3 shows some Pd/porous support composite membranes and their hydrogen permeation performance reported in literature and this work. It can be found that the thinner Pd membranes in the literature have higher hydrogen permeation flux but lower selectivity. The hydrogen permeation flux and selectivity of the Pd membranes in the literature which have the similar or even larger thicknesses are less than those in this work. Therefore, the M4 in this work exhibited an

Table 3 Pd/porous support composite membranes and their hydrogen permeation performance in literature and this work

Membrane	Deposition method	d_{Pd}/μm	T/°C	ΔP/kPa	J/(mol·m^{-2}·s^{-1})	H_2/N_2 selectivity	Source
Pd/Al_2O_3	ELP	6	500	100	0.265	58	[35]
Pd/Sil-1 zeolite/Al_2O_3	ELP	5	450	100	0.1	300	[36]
Pd/TS-1 zeolite/Al_2O_3	ELP	19	500	100	0.04	310	[37]
Pd/Al_2O_3/PSS	ELP	4.4	500	800	0.385	1124	[15]
Pd/pencil/PSS	ELP	7	450	100	0.24	120	[38]
Pd/CeO_2/PSS	ELP+DVC	6.4	500	100	0.235	565	[24]
Pd/CeO_2-OXI/PSS	ELP-PP	15.4	450	100−200	0.06−0.12	>10000	[25]
Pd/YSZ/PSS	ELP	27.7	450	100	0.06	∞	[10]
Pd/NaX/PSS	ELP	20	450	100	0.07	685	[39]
Pd/CeO_2/YSZ-Al_2O_3	ELP	14	500	100−700	0.12−0.55	14241−24960	This work

excellent balance between hydrogen permeation flux and selectivity as compared with other composite membranes in Table 3.

3.4 Thermal stability of Pd composite membranes

A further evaluation of thermal stability for the composite membranes was conducted by hydrogen permeation under controlled thermal conditions. Such evaluations have technical relevance, particularly concerning membranes during sustained operation with intermittent thermal cycling and a long-term operation. The thermal stability tests were performed for the M1 and M4. Figure 7 shows the permeation stability of the M1 and M4 during a thermal cycling between 350 and 500 °C. For each cycle, the hydrogen permeation tests were performed for 10 h at 350, 400, 450, and 500 °C, respectively. Following the above procedure, three cycles were sequentially performed up to ~120 h. It can be seen that the hydrogen permeation flux values of both composite membranes were generally stable during the cycles. The M1 and M4 can withstand a relatively high-temperature fluctuation without obvious damage of the Pd membranes.

Figure 8 shows the hydrogen permeation stability of the M1 and M4 during a thermal cycling between room temperature and 500 °C. For each cycle, the composite membranes were heated to 500 °C in N_2 atmosphere and the gas feed was switched to pure H_2 to determine the permeation flux, and then the N_2 permeation tests were performed after the hydrogen permeation tests to obtain selectivity. Finally, the system was cooled down to room temperature in N_2 atmosphere. Following the procedure, five cycles were sequentially performed with an operation time up to ~80 h. The hydrogen permeation flux through the M1 was slightly increased and the selectivity was

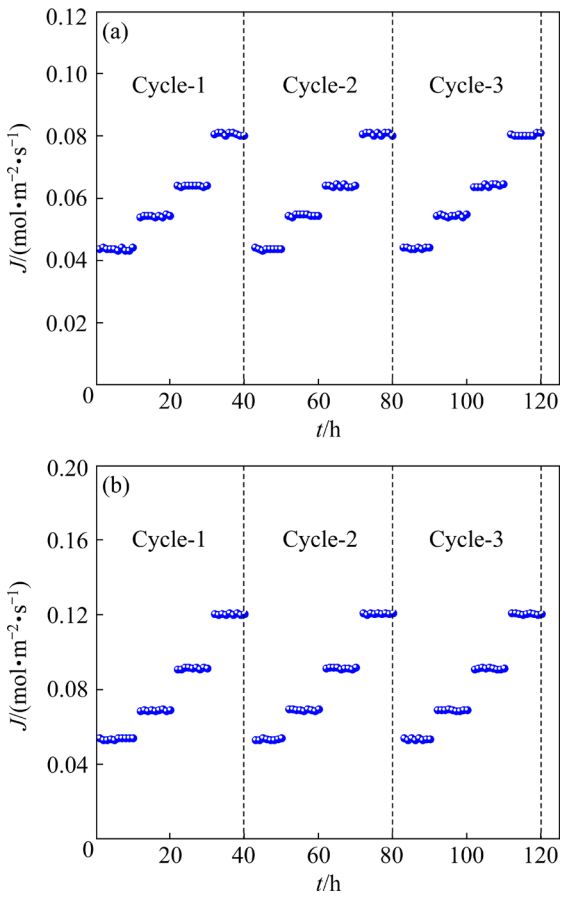

Fig. 7 Hydrogen permeation stability of M1 (a) and M4 (b) during thermal cycling between 350 and 500 °C under hydrogen pressure difference of 100 kPa

decreased from ~1018 to ~685, as shown in Fig. 8(a). The hydrogen permeation flux through M4 was generally the same and selectivity was stable at ~25000, as shown in Fig. 8(b). These indicate that the M4 remained intact and the M1 produced some defects. For the M4, the CeO_2 modification layer bridges the Pd membrane and the porous YSZ-Al_2O_3 tube. Since the thermal expansion coefficient of CeO_2 is similar to that of Pd, the CeO_2 layer provides suitable matching of thermal expansion between Pd membrane and YSZ-Al_2O_3 tube during thermal cycling. Thus, the M4 exhibited higher stability than the M1.

Figure 9 shows the permeation stability of the M1 and M4 during the long-term operation of 1000 h at 500 °C. It can be seen that the H_2 permeation flux and N_2 permeation flux through the M1 were gradually increased and those through the M4 remained stable over the long-term operation of 1000 h. The thermal stability of Pd composite membranes is related to a series of factors such as porous support, surface modification material, modification strategy, Pd deposition processes and operating conditions. Overall, the present results demonstrate that Pd membrane prepared on the porous YSZ-Al_2O_3 tube after the two-step CeO_2 modification exhibits an excellent thermal stability.

Figure 10 shows SEM images of the surface of Pd membranes in the M1 and M4 after long-term permeation tests. Compared with the as-prepared membrane (see Fig. 4(a)), the Pd membranes after tests exhibited coarse grains with larger sizes, wider grain boundaries and larger surface roughness, which are mainly attributed to the growth of Pd grains during permeation tests at evaluated temperatures. Specially, some pinholes can be seen on the surface of the Pd membrane in the M1, as shown in Figs. 10(a) and (b). These pinholes are the main reason for the poor stability of the M1, combined with the results of the thermal stability and long-term permeation tests. However, pinholes or defects did not appear on the surface of the Pd membrane in the M4, as shown in Figs. 10(c) and (d), which is consistent with the results of the thermal stability and long-term permeation tests of the M4. This might be related to the uniformity of Pd membrane microstructure for the Pd/CeO_2/YSZ-Al_2O_3 composite membranes.

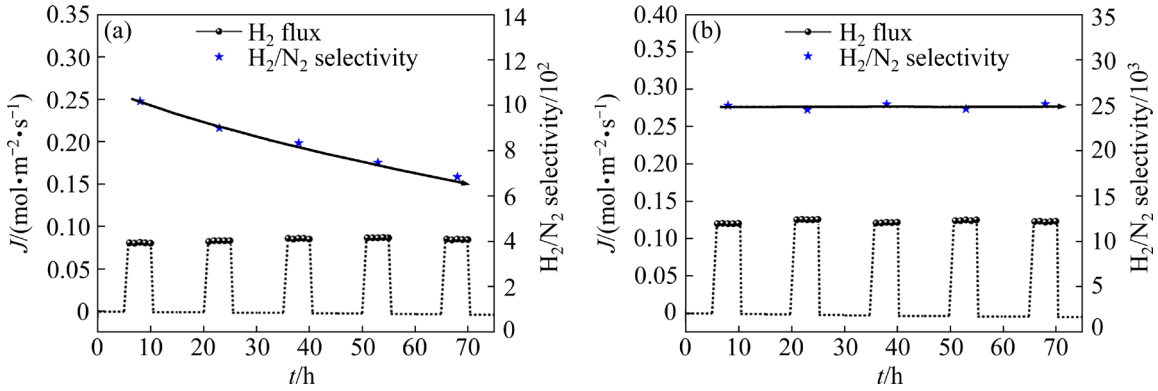

Fig. 8 Permeation stability of M1 (a) and M4 (b) during thermal cycling between room temperature and 500 °C under pressure difference of 100 kPa

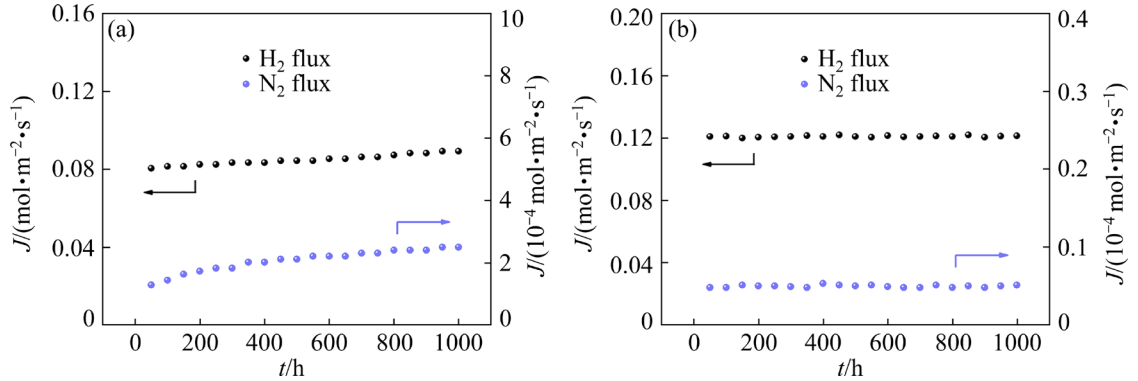

Fig. 9 Permeation stability of M1 (a) and M4 (b) at 500 °C under pressure difference of 100 kPa

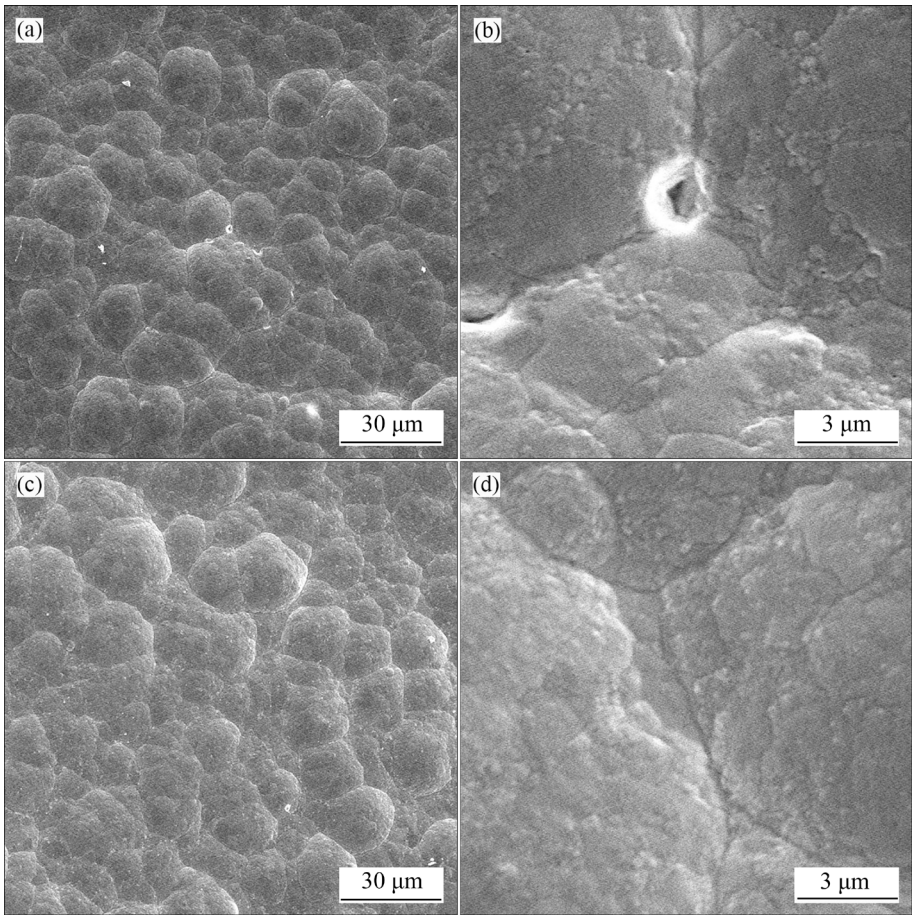

Fig. 10 SEM images of surface of Pd membranes in M1 (a, b) and M4 (c, d) after permeation tests

4 Conclusions

(1) Compared with no modification and the one-step CeO_2 modification, the surface of the porous YSZ-Al_2O_3 tubes after the two-step CeO_2 modification exhibited less defects, smaller pore distribution and roughness.

(2) Compared with different composite membranes, the Pd membranes on the porous YSZ-Al_2O_3 tubes after the two-step CeO_2 modification exhibited higher hydrogen permeation flux and H_2/N_2 selectivity. The highest hydrogen permeation flux was 0.549 $mol \cdot m^{-2} \cdot s^{-1}$ at 500 °C under a 700 kPa pressure difference, and the H_2/N_2 selectivity was 14241.

(3) The Pd membranes on the porous YSZ-Al_2O_3 tubes after the two-step CeO_2 modification exhibited high permeation stability during different thermal cycling tests and long-term permeation tests of 1000 h. This is because the CeO_2 layer provides suitable matching of thermal expansion between Pd membrane and YSZ-Al_2O_3 tube. The two-step CeO_2 modification has potential significance in the performance enhancement of Pd composite membranes.

Acknowledgments

The authors are grateful for the financial supports from the National Natural Science Foundation of China (Nos. 52171043, 51771066).

References

[1] PAGLIERI S N, WAY J D. Innovations in palladium membrane research [J]. Separation and Purification Methods, 2002, 31(1): 1−169.

[2] WANG You-bin, ZOU Rui, WEI Yue-zhou, ARAI T, FUJITA T. Electrochemical recycling of Pd and Ag from simulated high-level liquid waste [J]. Transactions of Nonferrous Metals Society of China, 2022, 32(3): 1031−1040.

[3] AL-MUFACHI N A, REES N V, STEINBERGER-WILKENS R. Hydrogen selective membranes: A review of palladium-based dense metal membranes [J]. Renewable and Sustainable Energy Reviews, 2015, 47: 540−551.

[4] UEMIYA S, SATO N, ANDO H, KUDE Y, MATSUDA T, KIKUCHI E. Separation of hydrogen through palladium thin film supported on a porous glass tube [J]. Journal of

Membrane Science, 1991, 56: 303−313.

[5] GIL A G, REISM H M, CHADWICK D, WU Z T, LI K. A highly permeable hollow fibre substrate for Pd/Al_2O_3 composite membranes in hydrogen permeation [J]. International Journal of Hydrogen Energy, 2015, 40(8): 3249−3258.

[6] KIADEHI D A, TAGHIZADEH M, RAMI M D. Preparation of Pd/SAPO-34/PSS composite membranes for hydrogen separation: Effect of crystallization time on the zeolite growth on PSS support [J]. Journal of Industrial and Engineering Chemistry, 2020, 81: 206−218.

[7] RYI S K, LEE S W, OH D K, SEO B S, PARK J W, PARK J S, LEE D W, KIM S S. Electroless plating of Pd after shielding the bottom of planar porous stainless steel for a highly stable hydrogen selective membrane [J]. Journal of Membrane Science, 2014, 467: 93−99.

[8] LI H, CARAVELLA A, XU H Y. Recent progress in Pd-based composite membranes [J]. Journal of Materials Chemistry A, 2016, 4(37): 14069−14094.

[9] YUN S, OYAMA S T. Correlations in palladium membranes for hydrogen separation: A review [J]. Journal of Membrane Science, 2011, 375: 28−45.

[10] SANZ R, CALLES J A, ALIQUE D, FURONES L, CORENGIA P, FERNANDEZ E. Preparation, testing and modelling of a hydrogen selective Pd/YSZ/SS composite membrane [J]. International Journal of Hydrogen Energy, 2011, 36(24): 15783−15793.

[11] FENG Li, ZHANG You-wei, WEN Chen, LI Si-zhen, LI Jia-feng, CHENG De, BAI Jing-ying, CUI Qing-xin, ZHANG Li-gong. Effect of initial deposition behavior on properties of electroless Ni−P coating on ZK60 and ME20 magnesium alloys [J]. Transactions of Nonferrous Metals Society of China, 2021, 31(8): 2307−2322.

[12] SANZ R, CALLES J A, ALIQUE D, FURONES L. New synthesis method of Pd membranes over tubular PSS supports via “pore-plating” for hydrogen separation processes [J]. International Journal of Hydrogen Energy, 2012, 37(23): 18476−18485.

[13] CHI Y H, LIN J J, LIN Y L, YANG C C, HUANG J H. Influence of the rotation rate of porous stainless steel tubes on electroless palladium deposition [J]. Journal of Membrane Science, 2015, 475: 259−265.

[14] MARDILOVICH I P, ENGWALL E, MA Y H. Dependence of hydrogen flux on the pore size and plating surface topology of asymmetric Pd-porous stainless steel membranes [J]. Desalination, 2002, 144: 85−89.

[15] CHI Y H, YEN P S, JENG M S, KO S T, LEE T C. Preparation of thin Pd membrane on porous stainless steel tubes modified by a two-step method [J]. International Journal of Hydrogen Energy, 2010, 35(12): 6303−6310.

[16] ZHENG L, LI H, XU H Y. “Defect-free” interlayer with a smooth surface and controlled pore-mouth size for thin and thermally stable Pd composite membranes [J]. International Journal of Hydrogen Energy, 2016, 41(2): 1002−1009.

[17] MEDRANO J A, FERNANDEZ E, MELENDEZ J, PARCO M, TANAKA D A P, ANNALAND M, GALLUCCI F. Pd-based metallic supported membranes: High-temperature stability and fluidized bed reactor testing [J]. International Journal of Hydrogen Energy, 2016, 41(20): 8706−8718.

[18] WANG D, TONG J H, XU H Y, MATSUMURA Y. Preparation of palladium membrane over porous stainless steel tube modified with zirconium oxide [J]. Catalysis Today, 2004, 93/94/95: 689−693.

[19] TARDITI A, GERBONI C, CORNAGLIA L. Pd−Au membranes supported on top of vacuum-assisted ZrO_2-modified porous stainless steel substrates [J]. Journal of Membrane Science, 2013, 428: 1−10.

[20] ZHANG K, GAO H Y, RUI Z B, LIU P, LI Y D, LIN Y S. High-temperature stability of palladium membranes on porous metal supports with different intermediate layers [J]. Industrial & Engineering Chemistry Research, 2009, 48: 1880−1886.

[21] HAWA H W, PAGLIERI S N, MORRIS C C, HARALE A, WAY J D. Application of a Pd−Ru composite membrane to hydrogen production in a high temperature membrane reactor [J]. Separation and Purification Technology, 2015, 147: 388−397.

[22] WEI Lei, YU Jian, HU Xiao-juan, HUANG Yan. Facile surface modification of porous stainless steel substrate with TiO_2 intermediate layer for fabrication of H_2-permeable composite palladium membranes [J]. Separation Science and Technology, 2016, 51(6): 998−1006.

[23] MOBARAKE M D, JAFARI P, IRANI M. Preparation of Pd-based membranes on Pd/TiO_2 modified NaX/PSS substrate for hydrogen separation: Design and optimization [J]. Microporous and Mesoporous Materials, 2016, 226: 369−377.

[24] TONG J H, SU C L, KURAOKA K, SUDA H, MATSUMURA Y. Preparation of thin Pd membrane on CeO_2-modified porous metal by a combined method of electroless plating and chemical vapor deposition [J]. Journal of Membrane Science, 2006, 269: 101−108.

[25] MARTINEZ-DIAZ D, SANZ R, CALLES J A, ALIQUE D. H_2 permeation increase of electroless pore-plated Pd/PSS membranes with CeO_2 intermediate barriers [J]. Separation and Purification Technology, 2019, 216: 16−24.

[26] MARTINEZ-DIAZ D, ALIQUE D, CALLES J A, SANZ R. Pd-thickness reduction in electroless pore-plated membranes by using doped-ceria as interlayer [J]. International Journal of Hydrogen Energy, 2020, 45(12): 7278−7289.

[27] SU C L, JIN T, KURAOKA K. Thin palladium film supported on SiO_2-modified porous stainless steel for a high-hydrogen-flux membrane [J]. Industrial & Engineering Chemistry Research, 2005, 44: 3053−3058.

[28] ALIQUE D, MARTINEZ-DIAZ D, SANZ R, CALLES J A. Review of supported Pd-based membranes preparation by electroless plating for ultra-pure hydrogen production [J]. Membranes, 2018, 8(1): 12−39.

[29] TERRA N M, BESSA L P, CARDOSO V L, REIS M H M. Graphite coating on alumina substrate for the fabrication of hydrogen selective membranes [J]. International Journal of Hydrogen Energy, 2018, 43(3): 1534−1544.

[30] HAN J Y, KIM C H, LIM H, LEE K Y, RYI S K. Diffusion barrier coating using a newly developed blowing coating method for a thermally stable Pd membrane deposited on porous stainless-steel support [J]. International Journal of Hydrogen Energy, 2017, 42(17): 12310−12319.

[31] MARDILOVICH P P, SHE Y, MA Y H. Defect-free palladium membranes on porous stainless-steel support [J]. AIChE Journal, 1998, 44(2): 310−322.
[32] WEI L, MA M X, LU Y H, WANG D S, ZHANG S L, WANG Q. Surface modification of macroporous Al_2O_3 tubes with carbon-doped TiO_2 intermediate layer and preparation of highly permeable palladium composite membranes for hydrogen separation [J]. Separation Science and Technology, 2020, 55(5): 980−987.
[33] GUAZZONE F, MA Y H. Leak growth mechanism in composite Pd membranes prepared by the electroless deposition method [J]. AIChE Journal, 2008, 54(2): 487−494.
[34] GUAZZONE F, PAYZANT E A, SPEAKMAN S A, MA Y H. Microstrains and stresses analysis in electroless deposited thin Pd films [J]. Industrial & Engineering Chemistry Research, 2006, 45: 8145−8153.
[35] GUO Y, WU H M, FAN X F, ZHOU L D, CHEN Q Q. Palladium composite membrane fabricated on rough porous alumina tube without intermediate layer for hydrogen separation [J]. International Journal of Hydrogen Energy, 2017, 42(15): 9958−9965.
[36] GUO Y, JIN Y J, WU H M, ZHOU L D, CHEN Q Q, ZHANG X F, LI X X. Preparation of palladium membrane on Pd/silicalite-1 zeolite particles modified macroporous alumina substrate for hydrogen separation [J]. International Journal of Hydrogen Energy, 2014, 39(36): 21044−21052.
[37] GUO Y, WU H M. Preparation of Pd-TS-1 composite membrane for hydrogen separation [J]. Advanced Materials Research, 2011, 299/300: 580−583.
[38] WEI L, YU J, HU X J, HUANG Y. Fabrication of H_2-permeable palladium membranes based on pencil-coated porous stainless steel substrate [J]. International Journal of Hydrogen Energy, 2012, 37(17): 13007−13012.
[39] MOBARAKE M D, SAMIEE L. Preparation of palladium/NaX/PSS membrane for hydrogen separation [J]. International Journal of Hydrogen Energy, 2016, 41(1): 79−86.

在两步 CeO_2 修饰的多孔 YSZ-Al_2O_3 管上制备高渗透性和热稳定性 Pd 膜

杨宇昕[1]，李新中[1,2]，梁 骁[2]，陈瑞润[1]，郭景杰[1]，傅恒志[1]，刘冬梅[3]

1. 哈尔滨工业大学 材料科学与工程学院，哈尔滨 150001；
2. 苏州大学 钢铁学院，苏州 215000；
3. Otto Schott Institute of Materials Research, Friedrich-Schiller-Universität Jena, Jena 07743, Germany

摘 要：采用化学镀技术在经过不同修饰方式后的多孔 YSZ-Al_2O_3 管上沉积 Pd 膜。采用 SEM、AFM、XRD 和气体渗透测试方法研究不同修饰方式对多孔 YSZ-Al_2O_3 管表面质量及 Pd 复合膜渗透性能的影响。结果表明，经两步 CeO_2 修饰后，多孔 YSZ-Al_2O_3 管表面具有更小的孔径分布和粗糙度。经两步 CeO_2 修饰后的多孔管上沉积的 Pd 膜在 500 ℃、700 kPa 压差下具有更高的氢渗透流量(0.549 $mol·m^{-2}·s^{-1}$)和 H_2/N_2 选择性(14241)。不同热循环测试和 1000 h 持久渗透测试结果表明，在经两步 CeO_2 修饰后的多孔管上沉积的 Pd 膜具有较高的渗透稳定性。

关键词：氢分离；Pd 膜；多孔管；表面修饰；CeO_2

(Edited by Wei-ping CHEN)